DOUBLE-BEAM AUTOCOMPENSATION FOR FLUORESCENCE POLARIZATION MEASUREMENTS IN FLOW CYTOMETRY

W. BEISKER AND W. G. EISERT
Gesellschaft fuer Strahlen- und Umweltforschung (GSF) Arbeitsgruppe Zytometrie, D-3000 Hannover 21, Federal Republic of Germany

ABSTRACT The degree of depolarization of fluorescent light emitted from an organic dye, which is used as molecular probe, is a powerful tool in probing the microenvironment. By fluorescence depolarization the macromolecular structure can be investigated as well as the the mobility of the marker molecule itself or of the complex formed by the probe. Additional information such as energy transfer rates, donor-acceptor distances, and orientations are also measurable. These data are of particular interest if they can be measured from whole cells. Using flow cytometry, we can analyze a large number of cells with high statistical significance in a short period of time. We describe a newly developed double-beam epi-illumination arrangement for fluorescence polarization measurements that uses an autocompensation technique. This new technique permits the various depolarizing effects within the optical as well as the electronic components of the system to be continually compensated for on a cell by cell basis. Simultaneous measurements of other cell parameters for cell cycle analysis by total fluorescence intensity remains possible. The sensitivity of the system to measure polarization was determined as $\pm$ 0.006 p ($0 \leq p \leq 0.5$ in isotropic media), which amounts to $\pm$ 1.2% of the maximum p value. Polarization data for latex microspheres plotted in the histogram mode were measured with a standard deviation of 0.006, which proved the high resolution and the high performance of the system.

INTRODUCTION

The microenvironment of the fluorescent marker molecules is probed by measuring the depolarization of fluorescence light. Molecular mobility in isotropic or anisotropic media (5, 16–18, 30), concentration effects (6, 18, 35), and molecular distances and/or orientations (2, 26, 29) may be investigated. This is of interest specifically in cell biology, where fluidity of cellular membranes as well as structure and conformation of nucleic acids (25, 35) are important. In contrast to measurements of fluorescence polarization of bulk cell suspensions in cuvettes, multiparameter investigations of single cells as done by flow cytometry permit a correlation of various parameters and polarization measurements with high statistical significance. An appropriate design of fluidics and optics of the flow cytometer permits optical and/or numerical compensation for depolarizing effects. Mismatch of optical and electronic components as well as anisotropic properties of mirrors and filters will give rise to systematic depolarization for various reasons. Epi-illumination and forward observation are favored over fluorescence polarization measurements at a right angle (19, 21) for theoretical reasons. The epi-illumination arrangement has been chosen to facilitate the extraction of fluorescent light from high background levels. Microscopic optics are highly desirable for high spatial resolution and high numerical aperture for low-level light detection. However, due to a high numerical aperture, various depolarization effects within the excitation and within the emission pathways have to be considered. This holds true even for selected optical components. In a previous paper we described the principles for the numerical correction of depolarizing effects. This correction was limited in its performance because a single-beam optical design was used (3, 9, 10). Here the overall performance and sensitivity of polarization measurements are improved. The double-beam optical design as described here allows various types of artifacts for each individual cell to be compensated for. This greatly improves the resolution and the accuracy of polarization measurements. A single cell is analyzed twice as it passes two parallel laser beams, the polarization vectors of which are orthogonal. A matrix algorithm for polarization measurements and subsequent compensation is described together with the appropriate experimental set-up. Applications in cell biology using DNA-specific dyes to study structural changes of the intracellular DNA are given as an example.

THEORETICAL EVALUATION OF THE AUTOCOMPENSATION TECHNIQUE

Various approaches for fluorescence depolarization measurements of individual cells using flow cytometric techniques have been published previously (1, 4, 13, 24, 29, 32). Due to its high stability and polarization ratio, a continuous laser source is desired for fluorescent polarization measurements. Small divergence of the laser beam simplifies the necessary optical arrangements. Operation in single transverse mode (TEM

00) resulting in a Gaussian intensity profile is highly desireable. The laser light beam will be highly linear polarized (up to a ratio of more than 1,000:1), if intracavity Brewster windows are used. Impurities and inhomogeneities of optical components (lenses, mirrors, etc.) will give rise to light scattering. This reduces the effective degree of polarization of the excitation light. The transmittance and reflectivity of dichroic mirrors must be carefully checked with respect to different polarization directions.

The polarization ratio will be gradually distorted along the optical axis for excitation and for emission by: (*a*) optical distortions appearing before the final focusing objective (scattering, anisotropic properties of optical components); (*b*) depolarization of light due to the numerical aperture of the objective (aperture depolarization); (*c*) influences of various refractive indices (Fresnel depolarization); (*d*) optical and electronical mismatch of the light detectors for the major directions of polarization (impaired sensitivity).

The depolarizing effects can be corrected by introducing a matrix algorithm as described previously (3, 9). The algorithm recalculates the actual polarization degree p in the sample from the distorted degree of polarization as recorded by photodetectors. The depolarizing factors for the excitation and emission pathways are given by matrices (A) and (B) as shown previously in reference 9. Matching the light detectors including subsequent electronic components is a necessary prerequisite. Any imbalance requires numerical compensation as is done by matrix (C). The algorithm was shown to be useful in compensating for a possible mismatch in a single beam design with two separate runs.

Instead of using two separate runs in a single beam arrangement, we compensated for a mismatch for each individual particle within the same run by using two separate beams. Cells passing two spatially separated excitation beams in a row will generate two pairs of data for fluorescence intensity components, which are parallel and perpendicular with respect to the direction of polarization of the excitation light. Although the two laser beams are spatially separated, fluorescence emission may be registered by the same set of photodetectors. Therefore, four intensity values will be registered for each particle or cell. The intensity values **D**, written as pseudovectors (3, 9) and measured by the two detector channels, may be written in a single beam system as: $\mathbf{D} = (C) * (B) * (A) * \mathbf{I}$. **I** represents the pseudovector of the laser emission, before the laser beam enters the optical system. In the following equations the indices 1 and 2 refer to the two laser-foci No. 1 and No. 2. Two equations for **D** and Q allow coefficients of (C) to be eliminated: $\mathbf{D}_1 = (C) * (B) * (\mathbf{F}_1) * Q$ (focus No. 1) and $\mathbf{D}_2 = (C) * (B) * (\mathbf{F}_2) * Q$ (focus No. 2) and $\mathbf{F}_1 = (A) * \mathbf{I}_1$, $\mathbf{F}_2 = (A) * \mathbf{I}_2$, and

$$Q = \begin{pmatrix} 1 \\ q \\ q \end{pmatrix}$$

with $q = 1 - p/1 + p$. The components of the vectors $\mathbf{F}_1$ or $\mathbf{F}_2$ form the matrix (F_i) or (F_2) as follow

$$(F_i) = \begin{pmatrix} f_{i1} & f_{i2} & f_{i3} \\ f_{i2} & f_{i3} & f_{i1} \\ f_{i3} & f_{i1} & f_{i2} \end{pmatrix} \text{ with } F_i = \begin{pmatrix} f_{i1} \\ f_{i2} \\ f_{i3} \end{pmatrix} \text{ and } i = 1 \text{ or } 2.$$

$\mathbf{I}_1$ and $\mathbf{I}_2$ represent the intensity pseudovectors of the different excitation foci (3, 9). Considering the approximation of a planar wave at the detector site (x components equal zero), four intensity components of $\mathbf{D}_1$ and $\mathbf{D}_2$ have to be measured. Assuming no cross talk between the two detector channels, matrix (C) will develop a diagonal form and the **Q** vector of true polarization degree can be evaluated.

All nonzero components of matrix (A) and (B) will equal unity, if a system shows no partial depolarization. As an example to show the algorithm, the equations will be given for the ideal nondepolarizing case

$$(A) = \begin{pmatrix} 0 & 0 & 0 \\ 0 & 1 & 0 \\ 0 & 0 & 1 \end{pmatrix} \qquad (B) = \begin{pmatrix} 0 & 0 & 0 \\ 0 & 1 & 0 \\ 0 & 0 & 1 \end{pmatrix}$$

$$\mathbf{I}_1 = \begin{pmatrix} 0 \\ 0 \\ 1 \end{pmatrix} \qquad \mathbf{I}_2 = \begin{pmatrix} 0 \\ 1 \\ 0 \end{pmatrix}$$

Vectors of the excitation intensity are

$$\mathbf{F}_1 = \begin{pmatrix} 0 \\ 0 \\ 1 \end{pmatrix} \quad \mathbf{F}_2 = \begin{pmatrix} 0 \\ 1 \\ 0 \end{pmatrix}.$$

The sensitivity matrix (C) may be given by

$$(C) = \begin{pmatrix} 0 & 0 & 0 \\ 0 & c_{22} & 0 \\ 0 & 0 & c_{33} \end{pmatrix}.$$

Therefore

$$\mathbf{D}_1 = \begin{pmatrix} 0 \\ d_{12} \\ d_{13} \end{pmatrix} = \begin{pmatrix} 0 \\ c_{22}q \\ c_{33} \end{pmatrix} \qquad \mathbf{D}_2 = \begin{pmatrix} 0 \\ d_{22} \\ d_{33} \end{pmatrix} = \begin{pmatrix} 0 \\ c_{22} \\ c_{33}q \end{pmatrix}$$

with q

$$q * q = \frac{(c_{22}\,q) * (c_{33}\,q)}{c_{22} * c_{33}} = \frac{d_{12} * d_{23}}{d_{13} * d_{22}}.$$

The polarization quotient q (or the polarization degree p) can now be determined by measuring the four intensities d_{12}, d_{13}, d_{22}, d_{23}; q therefore is independent of coefficients c_{22} and c_{33}. This implies that no further gain adjustment is necessary for the compensation.

EXPERIMENTAL SETUP

A schematic diagram of the optical concept is shown in Fig. 1. The laser beam of an argon-ion laser is split into two beams, which are polarized orthogonally to each other by the calcite crystal (CC). A polarization rotator (Spectra-Physics Inc., Mountain View, CA) in front of the crystal is used to adjust the intensity of the two beams. A cylindrical lens (z) and the planoconcave lens ($L1$) are used to generate astigmatic illumination of the entrance aperture. This results in different effective numerical apertures of the microscope objective (NA = 0.61; 4.1 mm focal length). A dichroic mirror ($M1$) separates the excitation beam from the fluorescent light. The cut-off edge at ~510 nm allows green and red fluorescent light (>510 nm) to be transmitted. The flow chamber with hydrodynamic focusing and double sheath-fluid system has previously been described by us (11, 12). A polarizing beam splitter separates two orthogonal polarized components of the fluorescent emission. The polarization axes of the polarizing beam splitter are aligned parallel to the polarization of the CC. Two photomultipliers (RCA 4840, extended red sensitivity; RCA, RCA New Products Div., Lancaster, PA) are used for fluorescence detection. Emission wavelength selection is achieved by interference filters as well as by long pass cut-off filters.

Parallel to the direction of flow the effective aperture is ~38° and 2.5° perpendicular to the flow. The aperture depolarization by the latter

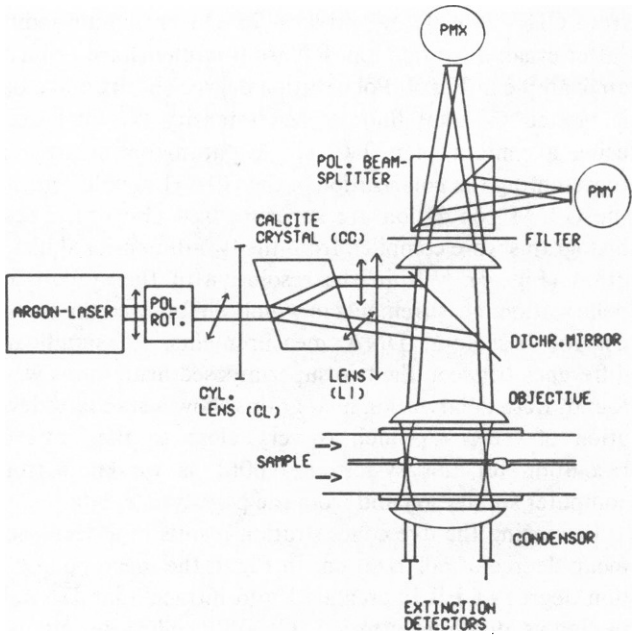

FIGURE 1 Schematic diagram of the double-beam optical design for fluorescence depolarization measurements in a flow cytometer.

(~2.5°) can be neglected. If water is used as the the outer sheath fluid and saline (0.9%) the inner fluid, the matrix (A) turns into

$$(A) = \begin{pmatrix} 0 & 0 & 0.01 \\ 0 & 0.410 & 0 \\ 0 & 0 & 0.402 \end{pmatrix}.$$

The intensity vectors $\mathbf{I}_1$ and $\mathbf{I}_2$ in the entrance pupil were measured as

$$\mathbf{I}_1 = \begin{pmatrix} 0 \\ 0.01 \\ 0.99 \end{pmatrix} \qquad \mathbf{I}_2 = \begin{pmatrix} 0 \\ 0.99 \\ 0.01 \end{pmatrix}.$$

This corresponds to a degree of polarization of 0.98. $\mathbf{F}_1$ and $\mathbf{F}_2$ are then

$$\mathbf{F}_1 = \begin{pmatrix} 0.024 \\ 0.010 \\ 0.966 \end{pmatrix} \qquad \mathbf{F}_2 = \begin{pmatrix} 0.000 \\ 0.990 \\ 0.010 \end{pmatrix}.$$

Assuming the full numerical aperture (0.61) of the objective matrix (B) is

$$(B) = \begin{pmatrix} 0 & 0 & 0 \\ 0.052 & 0.946 & 0.002 \\ 0.052 & 0.002 & 0.946 \end{pmatrix}.$$

The real polarization quotient q may be determined from the actually measured polarization quotient q' (given by d_{12}, d_{13}, d_{22}, d_{23}) by

$$q' = f(q) = \frac{0.0141 + 0.9880\,q}{0.9259 + 0.0316\,q}.$$

The conversion to the measured (p') and the true (p) degree of polarization is

$$p = \frac{0.228 + p'}{0.9534 + 0.0406\,p'}. \tag{1}$$

Fig. 2 shows a schematic diagram of the signal processing units. Signal output from the two photomultipliers are fed into two preamplifiers. A trigger and control logic in handshake mode with a Z-80 microcomputer (Tandy, Radio Shack TRS80/III; Fort Worth, TX) correlates the fluorescence pulses generated at each focus by using the extinction signals measured at each focus. Four maximum or integral decoders store pulse maxima or pulse integral values of the fluorescence intensity pulses, which are simultaneously converted by four analog-to-digital (A/D) converters (successive approximation; 8 bit).

During the course of a measurement the Z-80 microcomputer calculates the compensated value of the degree of polarization for each particle or cell using Eq. 1. Polarization data are stored either in a one-dimensional polarization histogram (256 channels) or combined with other parameters such as total fluorescence intensity, light scattering, extinction or particle size, in a two parameter histogram (64 × 64 channels) using the Z-80 microcomputer. The microcomputer system allows graphic histogram output as well as further numerical analysis.

Cell Culture, Preparation, and Staining

L1210 and HL-60 cells were kindly supplied by the Department of Hematology of the Medizinische Hochschule Hannover (MHH, Hannover; Federal Republic of Germany) and were cultured in RPMI 1640

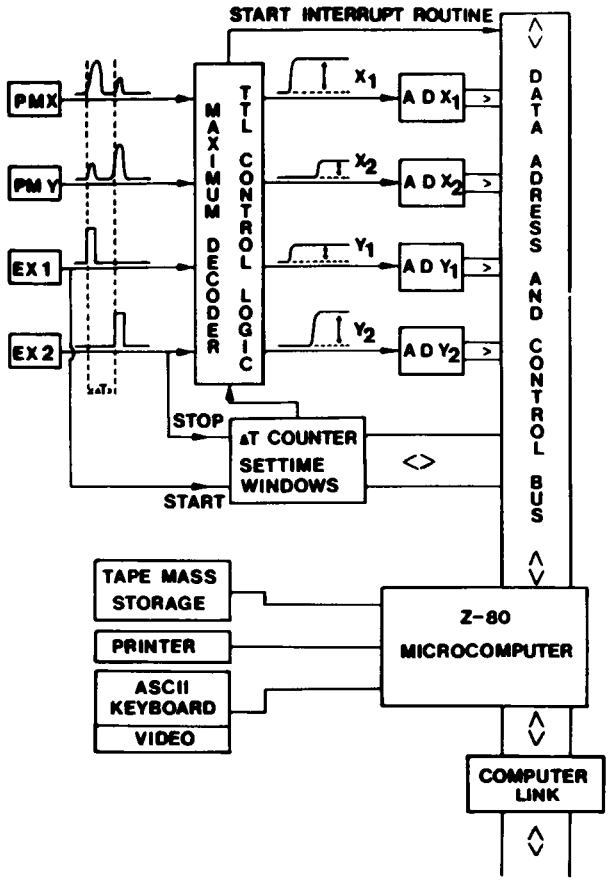

FIGURE 2 Schematic view of the electronic components used for signal processing within the double-beam autocompensation arrangement.

(Serva Fine Biochemicals, Inc., Garden City Park, NY, or Biochrom, West Berlin, Federal Republic of Germany) medium with 10% fetal bovine serum, 2% glutamine, and 1% amphotericine and neomycine. CH-V79 (Chinese hamster) were a gift from the Institut für Biophysikalische Strahlenforschung (GSF, Frankfurt, Federal Republic of Germany) and were cultured in L 5415 medium (Biochrom). The cells were harvested during logarithmic growth and fixed in 70% ethanol for ~1 d. After centrifugation cells were resuspended in phosphate buffered saline (PBS) to a concentration of $\sim 10^6$ cells/ml. RNase treatment (5,000 U/ml; Serva Fine Biochemicals, Inc. or Sigma Chemical Corp., St. Louis, MO) was done for 1 h at 37°. Cells were allowed to equilibrate in the dye solution for 10 min before the measurement (ethidium bromide [EB, Sigma Chemical Corp.] or propidium iodide [PI; Sigma Chemical Corp.] in PBS). Efficiency of the RNase treatment was monitored by the decrease of fluorescence intensity after additional DNase treatment.

RESULTS AND DISCUSSION

Fluorescent polystyrene microspheres are used to probe the resolution of the polarization measurements. Dye molecules exhibit very little mobility within the macromolecules. This results in a high degree of polarization. Fig. 3 shows a polarization histogram of fluorescent polystyrene microspheres (9.92 μm; Duke Scientific Corp., Palo Alto, CA). The mean value for the degree of polarization is $p = 0.395 \pm 0.006$ for ~10,000 particles being analyzed. A computer simulation of the polarization measurement including digitization errors of the 8 bit A/D converters results in a standard deviation of ~0.006. This confirms that the variation of ±0.006 p found in the microsphere experiment is the lower limit of resolution given the A/D conversion using 8-bit converters. Therefore a higher resolution can be achieved using 12- or 16 bit A/D converters. Fluorescence polarization of dye molecules intercalated into double-stranded nucleic acids such as acridine orange (AO), ethidium bromide (EB), and propidium iodide (PI) were analyzed during the cell-cycle progression. For each cell the degree of polarization and total fluorescence intensity were accumulated in a two parameter histogram. The proportionality of total fluorescence intensity to intracellular DNA is used to determine the phase of the cell cycle. Measurement using various cell lines (L1210, HL-60, CH-V79) gave similar results. Data from CH-V79 cells stained with 75 μM propidium iodide (after ethanol fixation and RNase treatment) are given as an example in Fig. 4. Polarization degree (horizontal axis) is plotted vs. total fluorescence intensity (vertical axis) using a contour plot. Two single parameter histograms representing the polarization of the G0/G1 population and the G2/M population are superimposed (Fig. 5). These histograms were compiled from the two-dimensional histogram (Fig. 4). Within the resolution of the system for polarization measurements in which we followed the protocol for best total DNA measurements, no significant difference between the two superimposed histograms were found. Both polarization histograms show a standard deviation of ±0.007, which is very close to the limit of resolution for this system (±0.006) as we know from computer simulation and from the polystyrene data.

Increasing the dye concentration results in a decreased mean degree of polarization. In Fig. 6 the mean polarization degree of EB intercalated into intracellular DNA is plotted vs. dye concentration (CH-V79 cells; after ethanol fixation and RNase treatment). Up to a concentration of ~60 μM EB the polarization degree decreases from 0.43 to ~0.27 (excitation 488 nm; emission >550 nm). This is correlated with a 10-fold increase of the fluorescence intensity as EB concentration increases from 1 to 60 μM. A similar relation was found for propidium iodide.

The properties of the intercalation process of EB or PI to DNA explain the strong decrease of the polarization degree with increasing dye concentration. Intercalation of EB or PI increases the quantum efficiency of the fluorescence emission quite strongly. Therefore, at higher concentrations further binding sites will be occupied (20, 22, 26, 33, 34, 37). Those nonintercalating binding sites do not increase fluorescence quantum yield with complex formation (20, 24, 37). Therefore even at high concentrations of dye molecules, the majority of photons are still emitted from intercalated dye molecules.

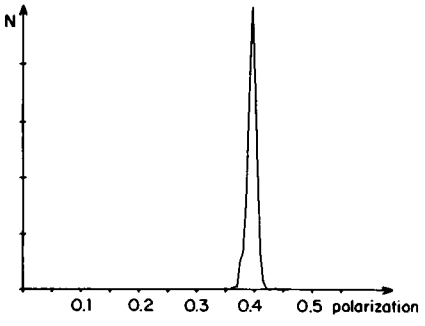

FIGURE 3 Fluorescence polarization one-dimensional histogram of fluorescent polystyrene microspheres (~10,000 particles analyzed). Excitation 488 nm, emission >550 nm. Mean degree of polarization, $p = 0.395 \pm 0.006$.

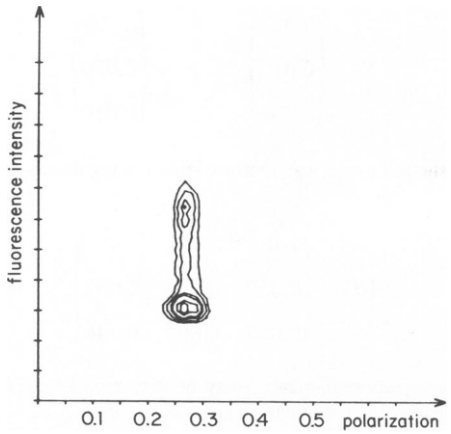

FIGURE 4 Degree of polarization vs. total fluorescence intensity (2-parameter contour plot) of PI (75 μmol) stained CH V79 cells. Excitation 488 nm, emission >550 nm, ~15,000 cells analyzed.

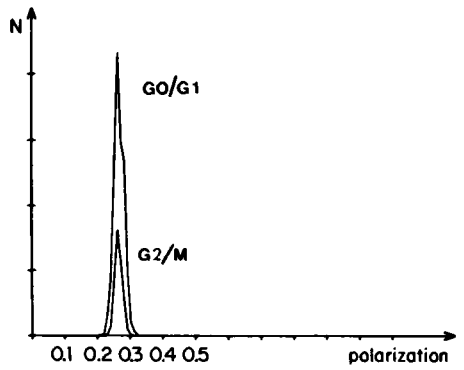

FIGURE 5 Two superimposed 1-parameter histograms of G0/G1 and G2/M phase as determined by total fluorescence intensity compiled from the same data set shown in Fig. 4.

Depolarization of fluorescent light may be explained differently by the rotation of the molecule during its fluorescent lifetime (14, 27, 35, 36) or by energy transfer between two dye molecules or between a dye molecule and other molecule in close proximity (14, 18, 25, 35, 36). At lowest dye concentration the energy transfer rate is assumed to be very small due to the large average distance between the intercalated dye molecules. A high degree of polarization at a low dye-phosphate ratio therefore indicates that binding of the dye molecule to the DNA double helix is rigid. At higher dye/phosphate ratios the decrease of the polarization can be explained by energy transfer between dye molecules binding at neighboring intercalating binding sites.

Comparing the results of EB-stained cells with naked DNA stained with EB, good agreement can be found. For the low concentration limit of EB-stained naked DNA, Wahl et al. (32) found a polarization degree of 0.42. At the high concentration limit our polarization values are slightly higher (0.27 compared with 0.19 found by Paoletti et al. in reference 25). A possible explanation may be that distorted energy transfer results from the influence of proteins at the cellular DNA.

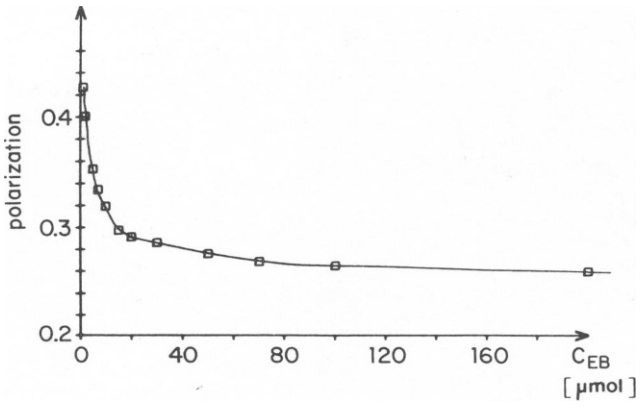

FIGURE 6 Influence of the concentration of dye (*PI*) on the degree of polarization of the fluorescent light. CH V79 cells. Excitation 488 nm, emission >550 nm.

CONCLUSION

A new flow cytometer for self-correcting fluorescence polarization measurements has been described. The unique double-beam autocompensation principle uses two sets of data to numerically compensate for a mismatch of the system on a cell-by-cell basis. With fluorescent microspheres the high resolution for polarization measurements (± 0.006 p) was shown. Mammalian cells stained with DNA-intercalating dyes, such as ethidium bromide and propidium iodide, were probed for fluorescence polarization. Energy transfer between dye molecules were dependent on dye molecule/phosphate ratios. Under staining conditions optimized for total DNA measurements no difference in the degree of fluorescence polarization was found during the cell cycle. This implies that the relative amount of DNA undergoing structural transition during the cell cycle either remains fairly constant or is too small to be detected under these experimental conditions. Further experiments will show to what extent treatment and/or improved staining protocols of DNA may amplify possible structural differences.

Received for publication 12 June 1984 and in final form 3 December 1984.

REFERENCES

1. Arndt-Jovin, D. J., and T. M. Jovin. 1976. Cell separation using fluorescence emission anisotropy. *In* Membranes and Neoplasia: New Approaches and Strategies. A. R. Liss, New York, 123–136.
2. Axelrod, D. 1979. Carbocyanine dye orientation in red cell membrane studied by microscopic fluorescence polarization. *Biophys. J.* 26:557–574.
3. Beisker, W., and W. B. Eisert. 1981. Principles of fluorescence polarization measurements. *Anal. Quant. Cytol.* 3:315–322.
4. Chan, S. S., D. J. Arndt-Jovin and T. M. Jovin. 1979. Proximity of lectin receptors on the cell surface measured by fluorescence energy transfer in a flow system. *J. Histochem. Cytochem.* 27:56–64.
5. Chu, Y. G., and C. R. Cantor. 1979. Segmental flexibility in *escherichia coli* ribosomal protein S1 as studied by fluorescence polarization. *Nucl. Acids Res.* 6:2363–2379.
6. Dale, R. E., and R. K. Bauer. 1971. Concentration depolarization of the fluorescence of dyestuffs in viscous solution. *Acta Phys. Pol.* A40:853–882.
7. Delbarre, A., M. I. Gourevitch, B. Gaugain, J. B. Le Pecq, and B. P. Roques. 1983. 1H NMR study of an ethidium dimer poly (dA-dT) complex: Evidence of a transition between bis and monointercalation. *Nucl. Acids Res.* 11(13:)4467–4482.
8. Eisert, W. G. 1981. High resolution optics combined with high spatial reproducibility in flow. *Cytometry.* 1(4):254–259.
9. Eisert, W. G., and W. Beisker. Epi-Illumination optical design for fluorescence polarization measurements in flow systems. *Biophys. J.* 31:97–112.
10. Eisert, W. G., W. Beisker, W. Hartmann and R. M. Eisert. Backward fluorescence detection in flow systems for the measurement of fluorescence emission anisotropy. Flow Cytometry IV. Universitetsforlaget, Bergen, Norway. 34–40.
11. Eisert, W. G., and M. Nezel. 1978. Internal calibration to absolute values in flowthrough particle size analysis. *Rev. Sci. Instr.* 49:1617–1621.
12. Eisert, W. G., R. Ostertag and E.-G. Niemann. 1975. Simple flow

microphotometer for rapid cell population analysis. *Rev. Sci. Instrum.* 46:1021–1024.

13. Epstein, M., A. Norman, D. Pinkel and R. Udkoff. 1977. Flow system fluorescence polarization measurements on fluorescein diacetate-stained EL4 cells. *J. Histochem. Cytochem.* 25:821–826.
14. Foerster, T. 1982. Fluoreszenz organischer Verbindungen. Vandenhoeck und Ruprecht, Göttingen, Federal Republic of Germany.
15. Hogan, M. E., and O. Jardetzky. 1980. Effect of ethidium bromide on DNA internal motions. *Biochemistry.* 19:2079–2085.
16. Jarry, J. P., and L. Monnerie. 1978. Orientation and molecular dynamics in uniaxial polymers. I. Theory of fluorescence polarization. *J. Polym. Sci. Part A-2.* 16:443–455.
17. Jarry, J. P., P. Sergot, C. Pambrun and L. Monnerie. 1978. A fluorescence polarization apparatus for the simultaneous measurement of orientation and mobility in unaxial media. *J. Phys. E. Sci. Instrum.* 11:702–706.
18. Jovin, T. M. 1979. Fluorescence polarization and energy transfer. Theory and application. *in* Flow Cytometry and Sorting. M. Melamed, P. Mullaney and M. Mendelsohn, editors. J. Wiley & Sons, Inc., New York. 137–165.
19. Kratohvil, J. P., M.-P. Lee and M. Kerker. 1978. Angular distribution of fluorescence from small particles. *Appl. Opt.* 17:1978–1980.
20. Le Pecq, J. B., and C. Paoletti. 1967. A fluorescent complex between ethidium bromide and nucleic acids. *J. Mol. Biol.* 27:87–106.
21. Lee, E.-H., R. E. Benner, J. B. Fenn and R. K. Chang. 1978. Angular distribution of fluorescence from monodispersed particles. *Appl. Opt.* 17:1980–1982.
22. Lerman, L. S. 1961. Structural considerations in the interaction of DNA and acridines. *J. Mol. Biol.* 3:18–30.
23. Lindmo, T., and H. B. Steen. 1977. Flow cytometric measurement of the polarization of fluorescence from intracellular fluorescein in mammalian cells. *Biophys. J.* 18:173–187.
24. Olmsted, J., III, and D. R. Kearns. 1977. Mechanism of ethidium bromide fluorescence enhancement on binding to nucleic acids. *Biochemistry.* 16:3647–3654.
25. Paoletti, J., and J. B. LePecq. 1971. Resonance energy transfer between EB molecules bound to nucleic acids. *J. Mol. Biol.* 59:43–62.
26. Paoletti, J., and J. B. LePecq. 1977. The structure of chromatin. Interaction of ethidium bromide with native and denatured chromatin. *Biochemistry.* 16(3):351–357.
27. Perrin, F. 1936. Diminution de la polarisation de la fluorescence des solutions resultant du movement Brownien de rotation. *Ann. Phys. Fr.* 335–347.
28. Price, G. B., M. J. McCutcheon, W. B. Taylor, and R. G. Miller. 1977. Measurement of cytoplasmic fluorescence depolarization of single cells in a flow system. *J. Histochem. Cytochem.* 25:597–600.
29. Ridler, P. J., and B. R. Jennings. 1980. Polarized fluorescence studies of electrically oriented DNA-dye solution. *Int. J. Biol. Macromol.* 2:313–317.
30. Tanaka, F., and N. Mataga. 1982. Dynamic depolarization of interacting fluorophores. *Biophys. J.* 39:129–140.
31. Udkoff, R., and A. Norman. 1979. Polarization of fluorescein fluorescence in single cells. *J. Histochem. Cytochem.* 27:49–55.
32. Wahl, P., C. Paoletti, and J. B. LePecq. 1970. Decay of fluorescence emission anisotropy of ethidium bromide-DNA complex. Evidence for an internal motion in DNA. *Proc. Natl. Acad. Sci. USA.* 65:417.
33. Wang, J., M. Hogan, and R. H. Austin. 1982. DNA motions in the nucleosome core particle. *Proc. Natl. Acad. Sci. USA.* 79:5896–5900.
34. Waring, M. J. 1965. Complex formation between EB and nucleic acids. *J. Mol. Biol.* 13:269–282.
35. Weber, G. 1952. Polarization of the fluorescence of macromolecules. *Biochemistry.* 51:145–157.
36. Weber, G. 1953. Rotational Brownian motion and polarization of the fluorescence of solutions. *Adv. Protein Chem.* 8:415–459.
37. Winkle, S. A., L. S. Rosenberg, and T. R. Krugh. 1982. On the cooperative and noncooperative binding of ethidium bromide to DNA. *Nuc. Acid Res.* 10(24):8211–8223.